ADVANCES IN ATMOSPHERIC SCIENCES, VOL. 31, JANUARY 2014, 118–130

The Impact of Global Warming on the Pacific Decadal Oscillation and the Possible Mechanism

FANG Changfang*[1,2], WU Lixin[1], and ZHANG Xiang[2]

[1]*Physical Oceanography Laboratory, Ocean University of China, Qingdao* 26600
[2]*Navy Marine Hydrometeorological Center of the Chinese PLA, Beijing* 100161

(Received 31 October 2012; revised 27 January 2013; accepted 4 March 2013)

ABSTRACT

The response of the Pacific Decadal Oscillation (PDO) to global warming according to the Fast Ocean Atmosphere Model (FOAM) and global warming comparison experiments of 11 IPCC AR4 models is investigated. The results show that North Pacific ocean decadal variability, its dominant mode (i.e., PDO), and atmospheric decadal variability, have become weaker under global warming, but with PDO shifting to a higher frequency. The SST decadal variability reduction maximum is shown to be in the subpolar North Pacific Ocean and western North Pacific (PDO center). The atmospheric decadal variability reduction maximum is over the PDO center.

It was also found that oceanic baroclinic Rossby waves play a key role in PDO dynamics, especially those in the subpolar ocean. As the frequency of ocean buoyancy increases under a warmer climate, oceanic baroclinic Rossby waves become faster, and the increase in their speed ratio in the high latitudes is much larger than in the low latitudes. The faster baroclinic Rossby waves can cause the PDO to shift to a higher frequency, and North Pacific decadal variability and PDO to become weaker.

Key words: Pacific Ocean, decadal variability, Pacific Decadal Oscillation, global warming, baroclinic Rossby waves

Citation: Fang, C. F., L. X. Wu, and X. Zhang, 2014: The impact of global warming on the Pacific Decadal Oscillation and the possible mechanism. *Adv. Atmos. Sci.*, **31**(1), 118–130, doi: 10.1007/s00376-013-2260-7.

1. Introduction

The Pacific Decadal Oscillation (PDO), as the dominant mode of North Pacific decadal variability, is characterized by a horseshoe-like SST anomaly, with a negative SST anomaly in the western and central North Pacific and a positive SST anomaly in the central and eastern equatorial Pacific, along the North American coast, and in the Gulf of Alaska (Fig. 1b). The PDO comprises two modes with approximate bidecadal (15–25 yr) and multidecadal (50–70 yr) periods, as indicated by the PDO index (Mantua et al., 1997), the 20th century North Pacific sea level pressure index (Minobe, 1999), and model simulation results (Latif and Barnett, 1994; Wu and Liu, 2003; Kwon and Deser, 2007; Zhong and Liu, 2009). In addition, the Hadley Centre Global Sea Ice and Sea Surface Temperature dataset (HadISST) (Rayner et al., 2003) PDO index (Fig. 1c) shows decadal to multidecadal power spectra (Fig. 1d), with spectrum peaks at about 50–70 and 15–25 yr.

A number of different mechanisms through which PDO modes are forced have been reported. For example, by the tropics through atmospheric teleconnection (Trenberth and Hurrell, 1994; Deser et al., 2004), by tropical and midlatitude interaction (Jacobs et al., 1994; Gu and Philander, 1997; Kleeman et al., 1999; Wu et al., 2007), by midlatitude local air–sea interaction (Latif and Barnett, 1996; Saravanan and McWilliams, 1998; Seager et al., 2001; Wu and Liu, 2003), and by midlatitude and subpolar interaction (Miller and Schneider, 2000; D'Orgeville and Peltier, 2009; Zhong and Liu, 2009). Regardless, for all of these PDO mechanisms, oceanic baroclinic Rossby wave adjustment plays a crucial role, and sets the PDO time scale.

The PDO has wide-ranging impacts on global climate, marine ecosystems and fisheries on the decadal time scale (Mantua et al., 1997; Mantua and Hare, 2002; Miller et al., 2004). In addition, as the decadal background, it can modulate seasonal and interannual climate variability, and is vital to short- and long-term climate prediction. The PDO influences ENSO onset and frequency (Wang, 1995; An and Wang, 1999), and enhances (cancels) ENSO climate teleconnections when they are in- (out-of-) phase (Gershunov and Barnett, 1998; Hu and Huang, 2009). The PDO also wields influence on summer rainfall patterns over China and America (Gershunov and Barnett, 1998, Huang et al., 2006). Overall, the PDO is an important element in the prediction of short- and long-term climate, marine ecology, and fisheries.

Global warming since the second Industrial Revolution

* Corresponding author: FANG Changfang
E-mail: fangchangfang@ 126.com

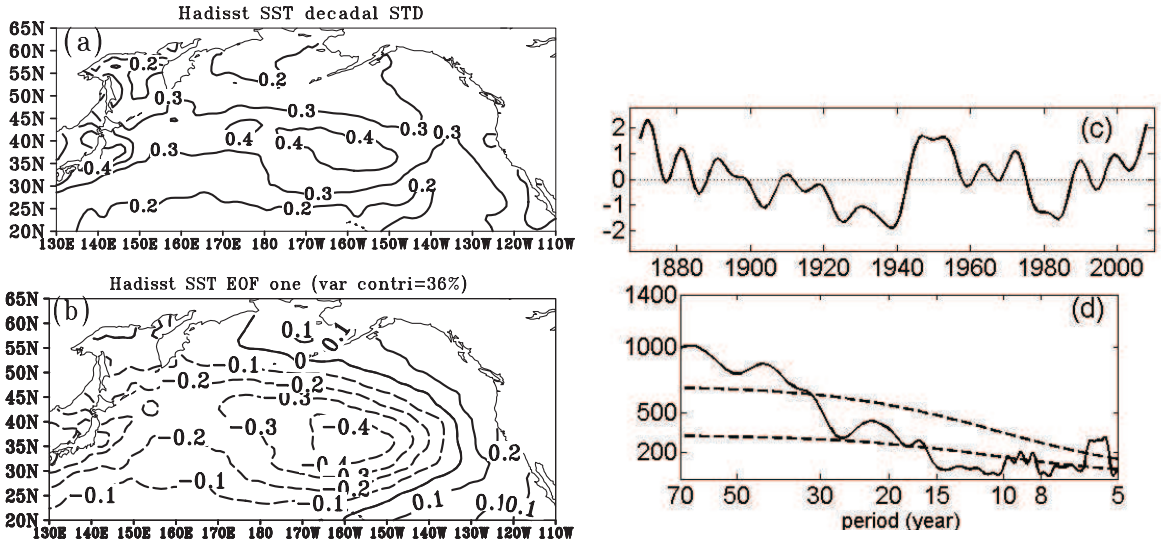

Fig. 1. (a) Hadisst SST decadal STD, (b) EOF first mode (units: °C), (c) standardized time coefficient series, and (d) the MTM raw power spectrum with 50% and 90% confidence level lines shown.

in the 1870s has led to persistent and irreversible climate changes. The impact of global warming (mean climate change) on climate variability has become a key scientific issue, as reflected by the establishment and efforts of organizations such as CLIVAR (Climate Variability and Predictability) and the IPCC. Work thus far using model ensemble simulations predicts a weaker Atlantic Meridional Overturning Circulation (AMOC) (Schmittner et al., 2005; Stouffer et al., 2006), but sufficient and reliable observations to verify these results are not available. The ENSO period might become shorter by 5%, but its amplitude change remains inconclusive (Merryfield, 2006; Guilyardi et al., 2009).

In the context of improving the climatic evaluation of global warming, as well as short- and long-term climate prediction, it is imperative to investigate the response of the PDO and the possible underlying mechanism. Superimposing decadal and interannual variability on the warming trend using historical instrumental data can only stretch back 100 years, so it is very difficult to separate decadal variability from the warming trend. Therefore, such data are insufficient for studying the PDO response to global warming, meaning we instead turn to paleoclimate data and global warming model simulations for greater insight. In paleoclimate research, northeastern Pacific tree-ring series and the reconstructed PDO index since 1700 A.D. have revealed evidence for less pronounced interdecadal variability after about the 1850s (D'Arrigo et al., 2001, Figs. 6 and 7). However, results based on other paleoclimate data are diverse (Mantua and Hare, 2002), and even opposite (Biondi et al., 2001). D'Orgeville and Peltier (2009) studied the PDO response to global warming using the low resolution version of the Community Climate System Model Version 3 (CCSM 3). In the 1870 control run, the PDO showed a typical period of about 20 years, determined by subpolar ocean processes in which salinity played an active role. When CO_2 concentration increased by 1% every year, with an integration length of 200 years, the typical 20-yr period could no longer be detected, and there was a larger multidecadal power spectrum. The disappearance of the 20-yr period was ascribed to the total melting of the Arctic ice cap, and speculation was made that global warming might modulate the PDO to a lower frequency (multidecadal period). However, their results were questionable. Their global warming spin-up run was only 200 years, with CO_2 concentration increasing by 1% every year, and the global climate did not reach equilibrium. Therefore, the larger multidecadal power spectrum might be a global warming residual caused by linear warming trend removal (Mann and Lees, 1996).

In the present study, the PDO response to global warming in the National Center for Atmospheric Research-Community Climate System Model Version 3 (NCAR_CCSM 3.0) IPCC Fourth Assessment Report (AR4) Picntrl and A1B experiments was investigated, and the results showed, as reported in section 4.2, the PDO getting weaker and shifting to a higher frequency under a warmer climate. We examined the PDO response to global warming in a double CO_2 equilibrium run of 400 years ($2CO_2$) and a corresponding control run of 400 years (Ctrl) (Table 1), so our results are more convincing. In addition, IPCC Picntrl and A1B simulations (Meehl et al., 2007) were used to validate the results. For most PDO mechanisms, the PDO time scale is set by the baroclinic Rossby wave speed (ocean adjustment process). Saenko (2006) conjectured that, under global warming, ocean stratification would enhance, Rossby waves would speed up, and the interannual and decadal variability periods might become shorter. Here, we report that global warming does indeed weaken the PDO and modulate it to a higher frequency.

The remainder of the paper is organized as follows. An introduction to the models used, the experiments, and anal-

Table 1. Global warming experiments used in the study.

Model	Experiment name	CO_2 concentration (ppm)	Experiment length
FOAM	Ctrl	355	400 years
	$2CO_2$	710	400 years
	PBnp	355	400 years
	PBstp	355	400 years
IPCC AR4 models	Picntrl	290	200 years
	A1B	Increase from 365 to 720	From 2000 to 2100
		720	From 2100 to future

ysis procedures are provided in section 2. Sections 3 and 4 present the results of the North Pacific decadal variability and PDO response to global warming, as simulated by the Fast Ocean Atmosphere Model (FOAM) and global warming simulations from eleven IPCC AR4 models. Section 5 elucidates the possible mechanism for the PDO response, and then a final discussion and conclusions are provided in section 6.

2. Methods

2.1. *Observation data, models and global warming experiments*

HadISST data from 1870 to 2010 with a resolution of $1^\circ \times 1^\circ$ (Rayner et al., 2003) were used to show the observed PDO spatial pattern and power spectrum. Details of the models and experiments used in the study are listed in Table 1. The main model used was the Fast Ocean Atmosphere Model, version 1.5 (FOAM1.5) (Jacob, 1997), which is a fully coupled ocean–atmosphere GCM without flux adjustment, consisting of atmosphere, ocean, land, ice and coupler components. FOAM has shown good performance in research on Pacific and Atlantic decadal variability, climate change and paleoclimate, as indicated at http://www.mcs.anl.gov/research/projects/foam/publications.html. In the FOAM control run of 400 years (Ctrl), greenhouse gas concentrations were fixed at 1990 levels, with a CO_2 concentration of 355 ppm. In the FOAM double-CO_2-equilibrium simulation ($2CO_2$), only the CO_2 concentration was doubled compared to Ctrl (i.e., at 710 ppm). The $2CO_2$ simulation was integrated for 760 years, with the last 400 years—during which the climate reached equilibrium—used for the analysis.

The IPCC's Picntrl (pre-industry experiment) and scenario A1B (global warming experiment) simulations are archived and provided by the Program for Climate Model Diagnosis and Intercomparison (PCMDI). The CO_2 concentration is fixed at 280 ppm in Picntrl. Under the A1B scenario, the CO_2 concentration is increased from 365 ppm in the year 2000 to 720 ppm by the year 2100, and remains constant thereafter. Eleven models with the A1B simulation extending to 2300 were selected to study North Pacific decadal standard deviation (section 3) and the PDO characteristic response to global warming. These were: NCAR_CCSM 3.0, CCCMA_CGCM3_1, CCMA_CGCM3_1_T63, CNRM_CM3, CSIRO_MK3_5, GFDL_CM2_0, GFDL_CM2_1, GISS_MODEL_E_R, MIROC3_2_MEDRES, MIUB_ECHO_G, and MRI_CGCM2_3_2A. The details of these models and experiments are introduced in the PCMDI website (http://www-pcmdi.llnl.gov/ipcc/model_documentation/ipcc_model_documentation.php).

In order to exclude the impact of the global warming trend, it is better to study the PDO response to global warming in stable climate equilibrium. The CO_2 concentration is fixed in the Ctrl, $2CO_2$ (the last 400 years), Picntrl, and A1B (from 2100) experiments, and so North Pacific decadal variability and the PDO response to global warming was studied (sections 3 and 4) between the FOAM Ctrl and $2CO_2$ experiments (both with 400-yr equilibrium climate), and between the Picntrl and A1B experiments. The magnitude of warming (CO_2 concentration increase) of the IPCC AR4 experiments (A1B minus Picntrl) is 440 ppm, which is larger than that (355 ppm) of the FOAM experiments ($2CO_2$ minus Ctrl), and so the baroclinic Rossby wave increase ratio is also more obvious in the IPCC AR4 models, as shown later in section 5.3.

2.2. *Partial blocking experiments*

Two Partial blocking (PB) experiments (Liu et al., 2002), namely PBnp and PBstp (Table 1), were carried out to investigate the role of oceanic baroclinic Rossby wave adjustment in the PDO, by comparison with Ctrl. The PBnp (PBstp) experiments were designed as follows. From 10° to 60°N (10° to 35°N), from 175° to 185°E, and at a depth of 100 m, ocean temperature and salinity are permanently fixed at the climatology. The North Pacific (subtropical North Pacific only) westward baroclinic Rossby waves were blocked and eliminated near the partial blocking region in PBnp (PBstp). Subpolar baroclinic Rossby waves still worked in PBstp.

2.3. *Analysis procedure*

The analysis procedure was the same for all variables in Figs. 1–8. Decadal variability in this study was generally regarded as variability with a period longer than eight years. Data procedures included the following four steps. (1) Winter annual mean (from October to the following March) time series were first linearly detrended to remove the warming trend and minor model drift. (2) Low-pass filtering ($>$ 8 yr) was performed to focus on the decadal variability. (3) The detrended and filtered field was then used to calculate the standard deviation (STD), derive the PDO mode and its time coefficient series through EOF analysis and Singular Value Decomposition (SVD) analysis. Grid variables were area-

weighted before EOF and SVD analysis. (4) The power spectrum of the PDO was calculated using a multitaper spectrum method (Mann and Lees, 1996). To exclude the nonphysical power peaks caused by filtering, the power spectrum was based on the unfiltered time coefficient obtained by projecting the derived PDO mode onto the unfiltered field derived in step (1) (Wu and Liu, 2003).

3. Response of North Pacific decadal variability to global warming

The detrended and low-pass filtered time series were used to calculate decadal STD. The SST STD and 500-hPa geopotential height (GPH) STD response to global warming are shown in Figs. 2 and 3, respectively.

3.1. *SST decadal STD change*

SST decadal STD in the observational HadISST data, as well as the FOAM and IPCC AR4 model control runs, is shown in Figs. 1a, 2a and 2b respectively, with the maximum in the western and central North Pacific, labeling the PDO center (Figs. 1b, 4a and 7a). From 20° to 50°N, the North Pacific SST decadal variability in FOAM (Fig. 2a) is overall consistent with that in the observation (Fig. 1a), with a maximum decadal STD of about 0.4°C. The ensemble mean of the IPCC AR4 models has much larger decadal variability, with a STD of 1°C in the Kuroshio-Oyashio Extension (KOE) region (Fig. 2b), compared to the observation and FOAM (Figs. 1a and 2a). The subpolar North Pacific ocean decadal variability in both FOAM and the IPCC AR4 models is larger than that in HadISST.

Under a warmer climate, North Pacific decadal variability (SST decadal STD) weakens in FOAM (Fig. 2c), the ensemble mean (Fig. 2d), and every one of the 10 IPCC AR4 models (not shown). North Pacific SST decadal STD decreases by 0.05°C–0.2°C (Figs. 2c and d), with a ratio of decrease from 10% to 40% (Figs. 2e and 2f). The North Pacific decadal variability reduction maximum is in the western and central North Pacific (PDO center) and subpolar North Pacific (especially the western subpolar North Pacific), implying a weaker PDO. Overall, as the latitude increases and longitude decreases in the North Pacific, the magnitude of SST decadal STD reduction and the reduction ratio increase, which might be related to the magnitude of ocean warming and the speed-up ratio of oceanic baroclinic Rossby waves (section 5.3). The magnitude of warming in the higher latitudes and in the west is larger than that in the lower latitudes and in the west (Fig. 9). The Rossby wave speed-up ratio in the high latitudes is larger than that in the low latitudes (Fig. 10).

When the climate warms, in the western half of the North Pacific, the magnitude of SST decadal variability reduction in FOAM (Fig. 2c) is almost equal to that in the IPCC AR4

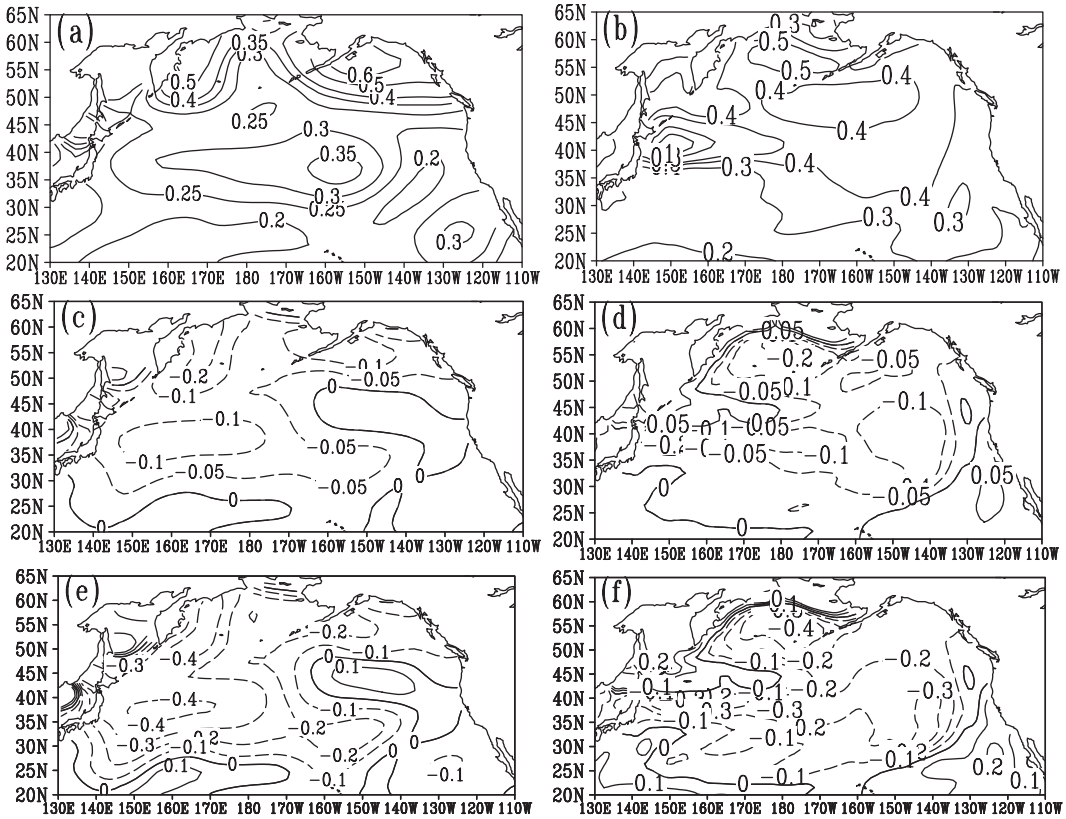

Fig. 2. SST decadal STD (units: °C) (a, b) in Ctrl and Picntrl, its change (c, d) under global warming, and the change ratio (e, f), in FOAM (left column) and 10 IPCC AR4 models (right column).

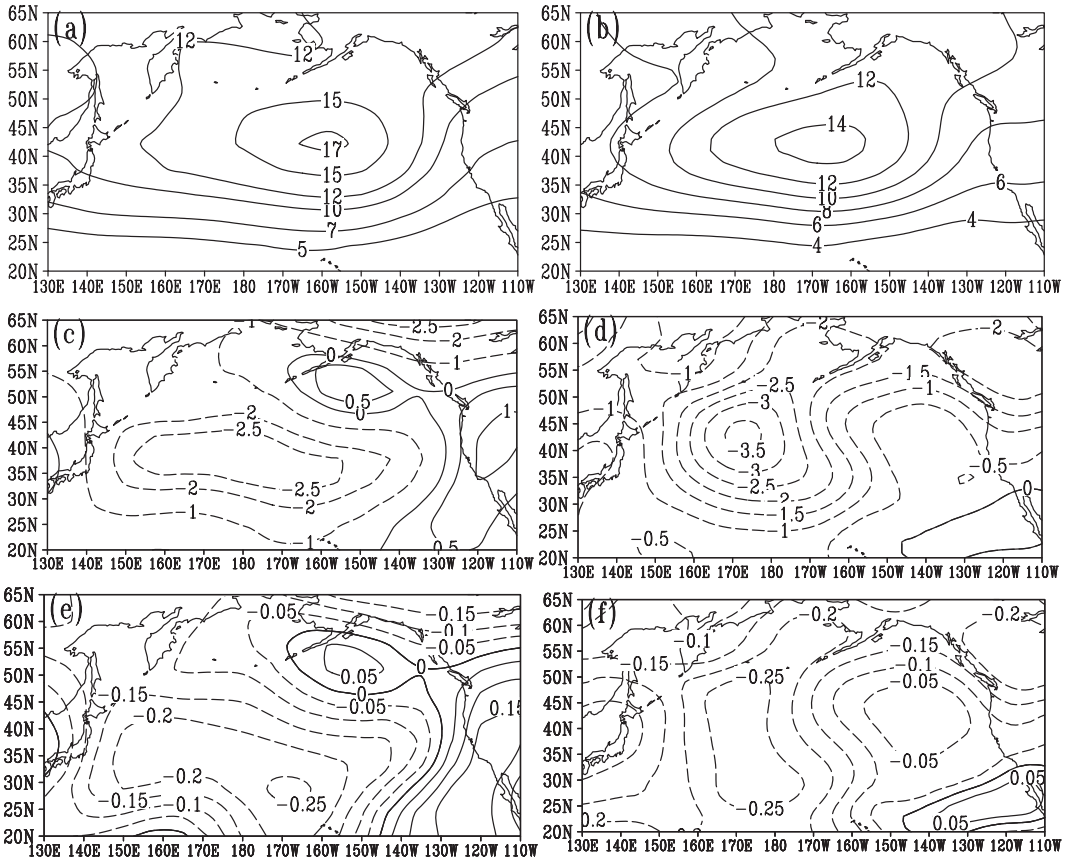

Fig. 3. 500-hPa GPH decadal STD (units: m) (a, b) in Ctrl and Picntrl, its change (c, d) under global warming, and the change ratio (e, f), in FOAM (left column) and 10 IPCC AR4 models (right column).

models (Fig. 2d), with 0.1°C in the KOE region and 0.2°C in the western subpolar region. Since the IPCC AR4 models have a larger decadal variability in the KOE region (mentioned above), the SST decadal variability reduction ratio in the FOAM KOE region (western North Pacific) is a little larger than that in the IPCC AR4 models (Figs. 2e and f). Incidentally, global warming might shift mid-latitude storm tracks and the KOE northward (Yin, 2005; Sato et al., 2006), so there is a regional gap of minor SST decadal STD increase in the north of the KOE in the IPCC AR4 model results (Figs. 2d and f).

3.2. *500-hPa GPH decadal STD change*

For 500-hPa GPH, the results for the IPCC AR4 models is the ensemble mean of five IPCC AR4 models with available Picntrl and A1B data; namely, CCCMA_CGCM3_1, CCMA_CGCM3_1_T63, CSIRO_MK3_5, GFDL_CM2_0, and GFDL_CM2_1. Similar to North Pacific Ocean decadal variability, North Pacific atmosphere decadal variability also weakens in response to global warming (Fig. 3). In FOAM and IPCC AR4 model control runs, 500-hPa GPH decadal STD maxima are all over the PDO center (Figs. 3a and b). North Pacific 500-hPa GPH decadal STD reduces under global warming (Figs. 3c and d) by 5%–25% (Figs. 3e and f). The 500-hPa GPH decadal STD reduction maximum is also over the western North Pacific, consistent with the SST decadal STD reduction maximum. The 850-hPa and 250-hPa GPH decadal variability response to global warming is similar to the 500-hPa GPH response (not shown).

Overall, North Pacific Ocean and atmosphere decadal variability weaken under global warming. The ocean decadal variability weakening maximum is in the western North Pacific Ocean (PDO center) and subpolar North Pacific Ocean. The atmosphere decadal variability weakening maximum is mainly over the western North Pacific Ocean (PDO center). The following section further validates this result of a weaker PDO under global warming.

4. PDO amplitude and frequency response to global warming

This section reports the results from studying the effect of global warming on PDO spatial structure and frequency (period). The PDO is the dominant mode (EOF mode one) of North Pacific SST, upper ocean heat content and 500-hPa GPH decadal variability, in both FOAM and the IPCC AR4 models.

4.1. *PDO change in FOAM*

PDO spatial structure in FOAM (Figs. 4a and d) is consistent with that in the observation (Fig. 1b) and other model

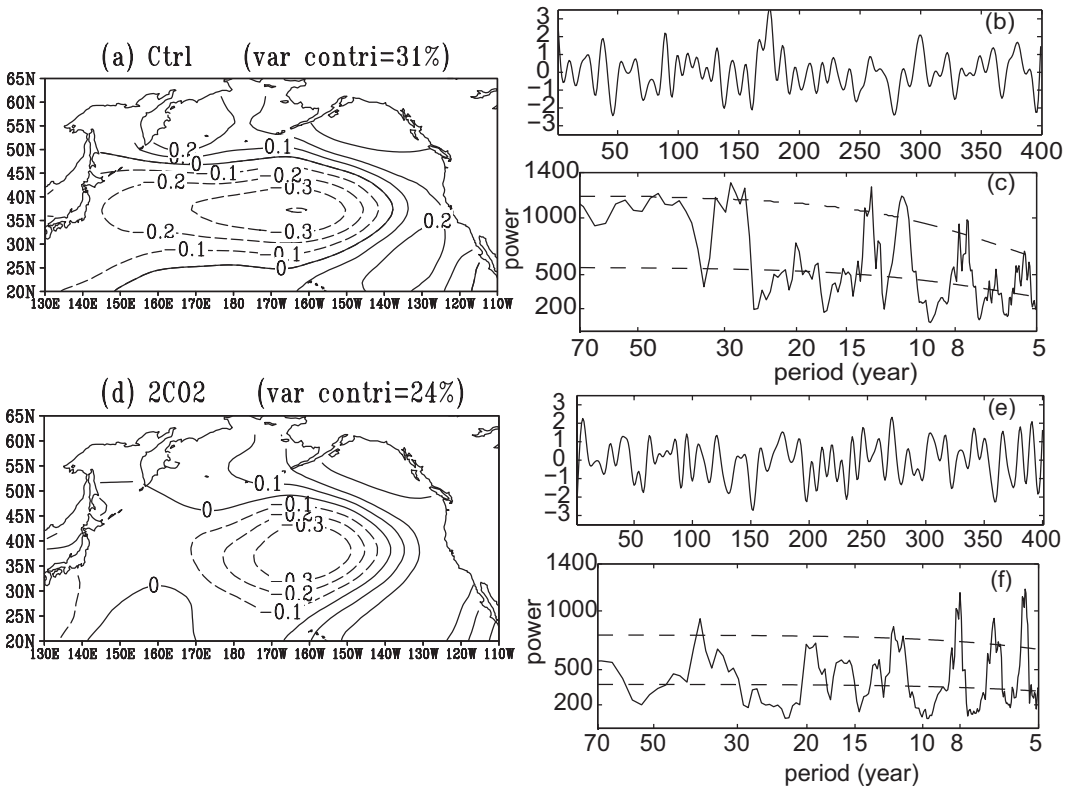

Fig. 4. (a) SST EOF first mode (units: °C), (b) the standardized time coefficient series, and the (c) MTM raw power spectrum with the 50% and 90% significance level lines shown in FOAM Ctrl. (d–f) The same as (a–c), but for FOAM $2CO_2$.

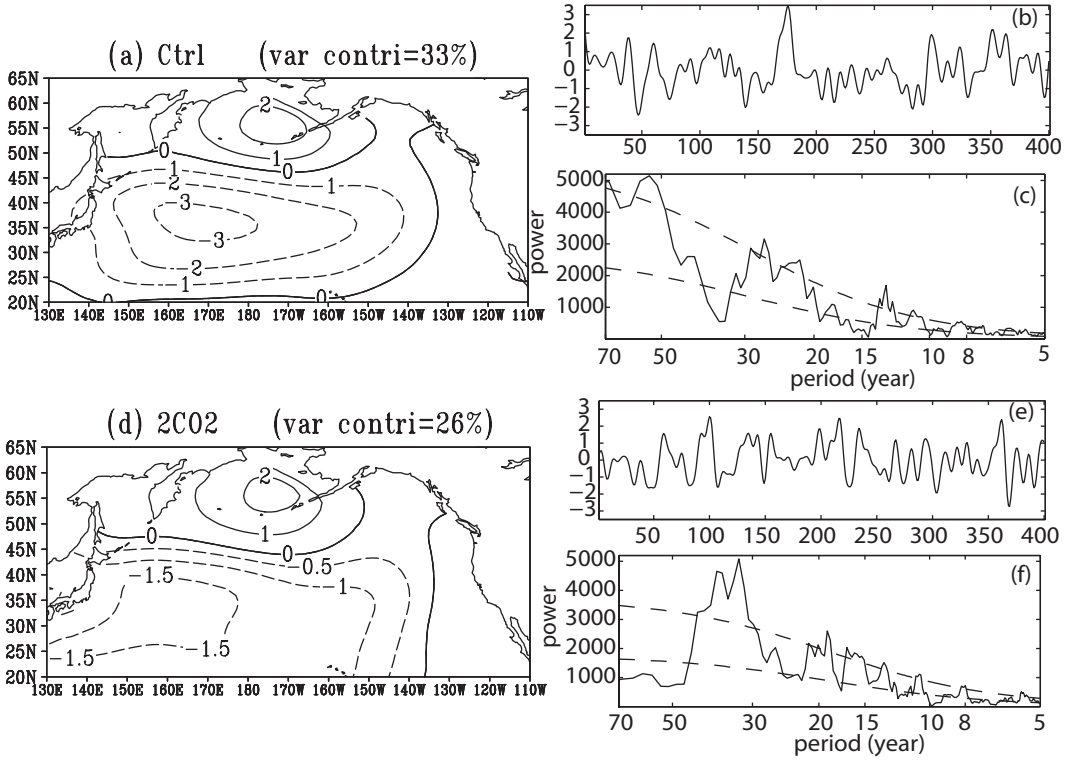

Fig. 5. The same as Fig. 4, but for upper-ocean (400 m) heat content (units: 10^8 J m^{-2}).

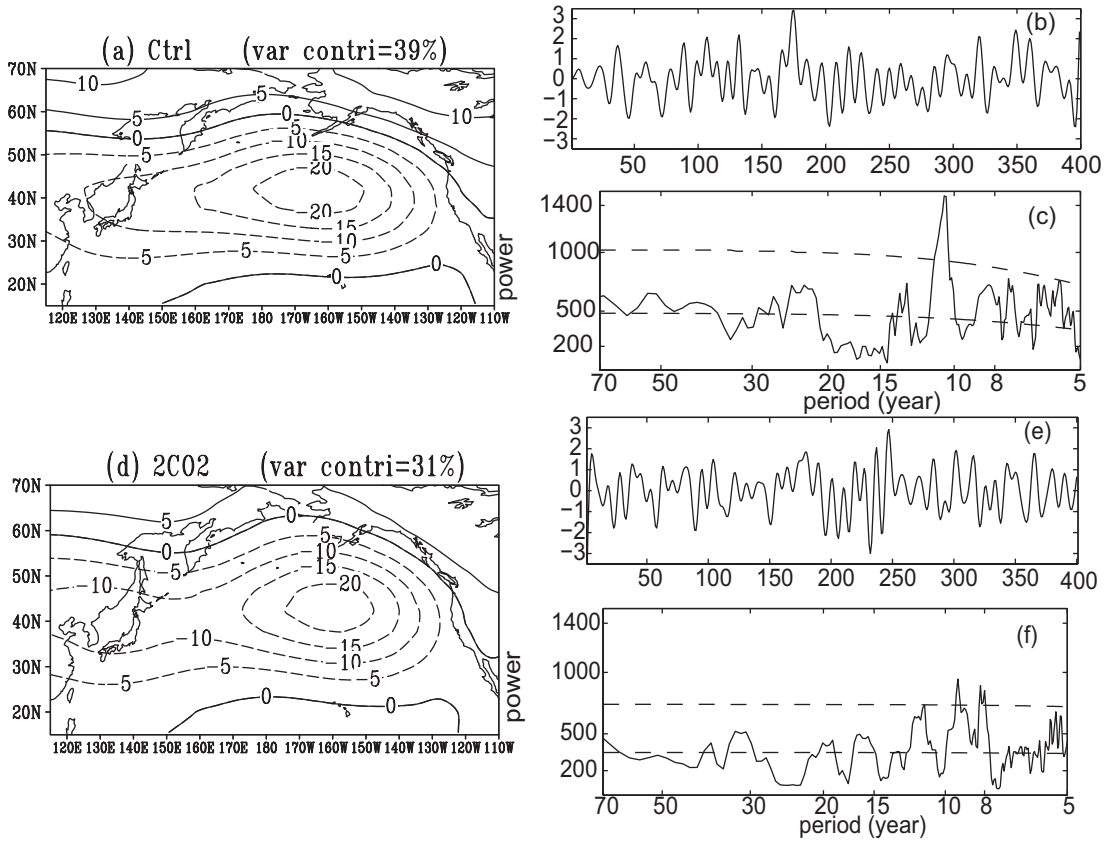

Fig. 6. The same as Fig. 4, but for 500-hPa GPH (units: m).

results (Figs. 7a and d): SST changes out-of-phase between the western and central North Pacific and the surrounding region. The PDO power spectrum in FOAM (Fig. 4c) shows substantial variance at decadal to multidecadal time scales, with two peaks at about 11–15 years and 30–70 years (Wu and Liu, 2003). Under a warmer climate ($2CO_2$ compared with Ctrl), the SST amplitude of the PDO weakens significantly, from 0.2°C to 0.05°C in the western North Pacific (Figs. 4a and d). The decadal to multidecadal spectra peaks all decrease significantly (Figs. 4c and f). In contrast, the interannual frequency power spectrum increases. The variance contribution of the PDO mode (SST first EOF mode) to North Pacific decadal variability decreases from 31% in Ctrl to 24% in $2CO_2$. Therefore, global warming weakens the PDO and shifts it to a higher frequency.

The PDO is not only a sea-surface phenomenon, but also an upper-ocean and atmosphere decadal variability dominant mode. The effect of global warming on the PDO is further validated and more clearly presented by upper-ocean (400 m) heat-content dominant mode change (Fig. 5): the maximum center in the western and central North Pacific weakens by 50% (form 3×10^8 to 1.5×10^8 J m^{-2}); the peaks in the time coefficient series get closer in $2CO_2$ compared to Ctrl (Figs. 5b and e); and the power spectrum peaks shift to a higher frequency (the dominant periods shorten) (Figs. 5c and f). The variance contribution of the PDO heat content mode decreases from 33% in Ctrl to 26% in $2CO_2$.

As the counterpart of the PDO in the ocean (Fig. 4), the dominant decadal mode of North Pacific 500-hPa GPH (Figs. 6a and c) is characterized by a negative anomaly in the western and central North Pacific and a surrounding positive anomaly, with a dominant period of about 11 years. Consistent with the SST and heat content dominant mode changes, the 500-hPa GPH dominant mode also weakens and shifts to a higher frequency under global warming (Fig. 6). GPH over the western and central north Pacific decreases by 2–3 m and the 11-yr power spectrum peak disappears. The variance contribution of the 500-hPa GPH first EOF mode decreases from 39% in Ctrl to 31% in $2CO_2$. The SVD first modes (the ocean–atmosphere coupled PDO mode) between SST and surface wind, and between SST and 500-hPa GPH, also weaken and shift to the higher frequency (not shown).

In conclusion, the dominant modes of North Pacific Ocean decadal variability (PDO) and North Pacific atmosphere decadal variability weaken and the PDO shifts to a higher frequency in the FOAM global warming comparison experiments.

4.2. *PDO change in the IPCC AR4 models*

Overall, the IPCC AR4 model results are consistent with those of FOAM. Two hundred years' data in Picntrl and A1B (from year 2101 to 2300, or from year 2150 to 2349) were used to study the PDO response to global warming. Eight of the 11 selected IPCC AR4

models showed the PDO getting weaker and shifting to a higher frequency under a warmer climate; namely, NCAR_CCSM 3.0, GFDL_CM2_0, GFDL_CM2_1, CCCMA_CGCM3_1, CCMA_CGCM3_1_T63, CNRM_CM3, MIROC3_2_MEDRES and MIUB_ECHO_G.

Since NCAR_CCSM 3.0 has the longest extension of A1B experiment simulation data (to the year 2349), we focus on its results here. Figure 7 shows the PDO response to global warming in the NCAR_CCSM 3.0 Picntrl and A1B experiments (both are from the year 2150 to 2349). The PDO in the NCAR_CCSM 3.0 Picntrl experiment (Fig. 7a) has a similar spatial pattern to that in the observation (Fig. 1b) and FOAM (Fig. 4a), but the SST magnitude in the KOE region is a little larger. The PDO periods are about 10–15 years and 20–30 years (Fig. 7c). Under a warmer climate (A1B scenario), the PDO amplitude gets weaker in the western North Pacific Ocean (Figs. 7a and d), and the spectrum peaks decrease and shift to a higher frequency (Figs. 7c and f). Compared to that in Picntrl, it is clear that the time coefficient series gets closer in A1B, indicating shorter periods. The variance contribution of the PDO mode (SST first EOF mode) to North Pacific decadal variability decreases from 46% in Picntrl to 39% in A1B.

Both FOAM and the eight IPCC AR4 model experiment results show that global warming weakens the PDO and shifts it to a higher frequency, with the PDO maximum weakening center in the western North Pacific. The following section investigates the relationship between the change in speed of oceanic baroclinic Rossby waves and the PDO response to global warming.

5. Rossby wave speed and the response of the PDO to global warming

5.1. *The role of baroclinic Rossby waves in the PDO*

Oceanic baroclinic Rossby waves represent one of the dominant ways through which the ocean adjusts over long time scales (months to decades), determining the period of ocean variability. There are many PDO mechanisms, which may play a role individually or collectively. However, ocean adjustment through baroclinic Rossby waves is the critical process in many PDO mechanisms (Latif and Barnett, 1996; Münnich et al., 1998; Kleeman et al., 1999; Pierce et al., 2001; Seager et al., 2001; Kwon and Deser, 2007; D'Orgeville and Peltier, 2009; Zhong and Liu, 2009). Thus, the role of North Pacific baroclinic Rossby waves in the PDO and its response to global warming were investigated, the results of which are reported below in sections 5.2 and 5.3. Section 5.4 then provides a conclusion to this part of the study.

5.2. *Results of the PBnp and PBstp experiments*

Figure 8 shows the SST dominant modes and multi-taper method (MTM) spectra in PBnp and PBstp. No North Pacific baroclinic Rossby waves were applied in Pbnp, and only subpolar North Pacific baroclinic Rossby waves (35°–60°N) were applied in Pbstp. Compared to the counterpart in Ctrl (Fig. 4), the PBnp SST dominant mode weakens obviously in the western and central North Pacific and subpolar North Pacific, and its decadal power spectrum decreases significantly to below the 90% confidence level, suggesting no PDO without North Pacific baroclinic Rossby waves. With only subpolar North Pacific baroclinic Rossby waves, the Pbstp SST dominant mode also weakens in the western and central North Pacific, but its two decadal power spectrum peaks (bidecadal and multidecadal) still exist and show no obvious change. The PBnp and PBstp experiments suggest that North Pacific baroclinic Rossby waves, especially subpolar North Pacific baroclinic Rossby waves (35°–60°N), are vital to the PDO (including two PDO modes, bidecadal and multidecadal). The study by Zhong and Liu (2009) also demonstrated that subpolar North Pacific Rossby waves are critical for Pacific multidecadal variability.

The PDO SST amplitude in PBnp (Fig. 8a) and PBstp (Fig. 8d) is less than that in Ctrl (Fig. 4a), and that in Pbnp is less than that in PBstp, indicating the role of North Pacific Ocean baroclinic Rossby wave adjustment in the PDO SST amplitude. Therefore, when oceanic baroclinic Rossby waves speed up under global warming, the PDO SST amplitude will decrease (Figs. 4a and d). Overall, North Pacific Ocean baroclinic Rossby waves are important to both the PDO period and PDO SST amplitude.

5.3. *Change in Baroclinic Rossby wave speed under global warming*

This section presents the results of changes in baroclinic Rossby waves with and without consideration of background mean current. Without considering background mean current, in absence of buoyancy forcing, wind stress and frictional forces, the standard linear theory for freely propagating linear waves gives the *m*-order baroclinic Rossby wave phase speed poleward of 5° (Chelton et al., 1998):

$$C_{mx} = -\beta\lambda_m^2 = -\beta\left(\frac{1}{m\pi|f|}\int_{-H}^{0} N(z)dz\right)^2 \quad m \geqslant 1, \quad (1)$$

where m is the order number, f is the Coriolis parameter, $\beta = \partial f/\partial y, \lambda_m$ is the m-order baroclinic Rossby wave deformation radius, $N(z)$ is buoyancy frequency and H is local ocean depth. According to Eq. (1), baroclinic Rossby wave phase speed is proportional to the square of buoyancy frequency integration along depth, and inversely proportional to the square of the order number m.

However, the observed first baroclinic Rossby wave speed according to TOPEX/POSEIDON satellite altimeter data was found to be faster than the theoretical result (Chelton and Schlax, 1996), suggesting a deficiency in the standard linear theory. Further, when baroclinic zonal mean flow is taken into account and the meridional potential vorticity gradient is modified (Killworth et al., 1997), discrepancy between observed speed and theoretical speed decreases:

$$(u-c)W_{zz} - u_z W_z + \frac{\beta N^2}{f^2}W = 0, \quad (2)$$

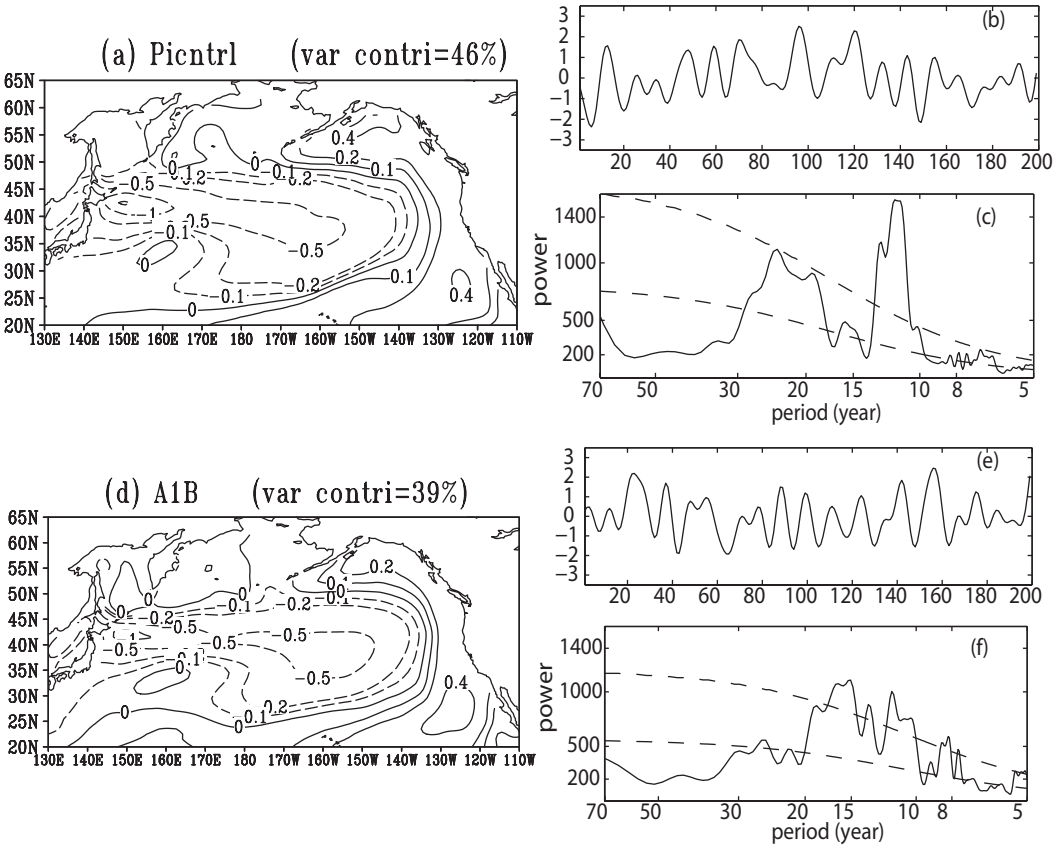

Fig. 7. The same as Fig. 4, but for SST in the NCAR_CCSM 3.0 Picntrl and A1B experiments.

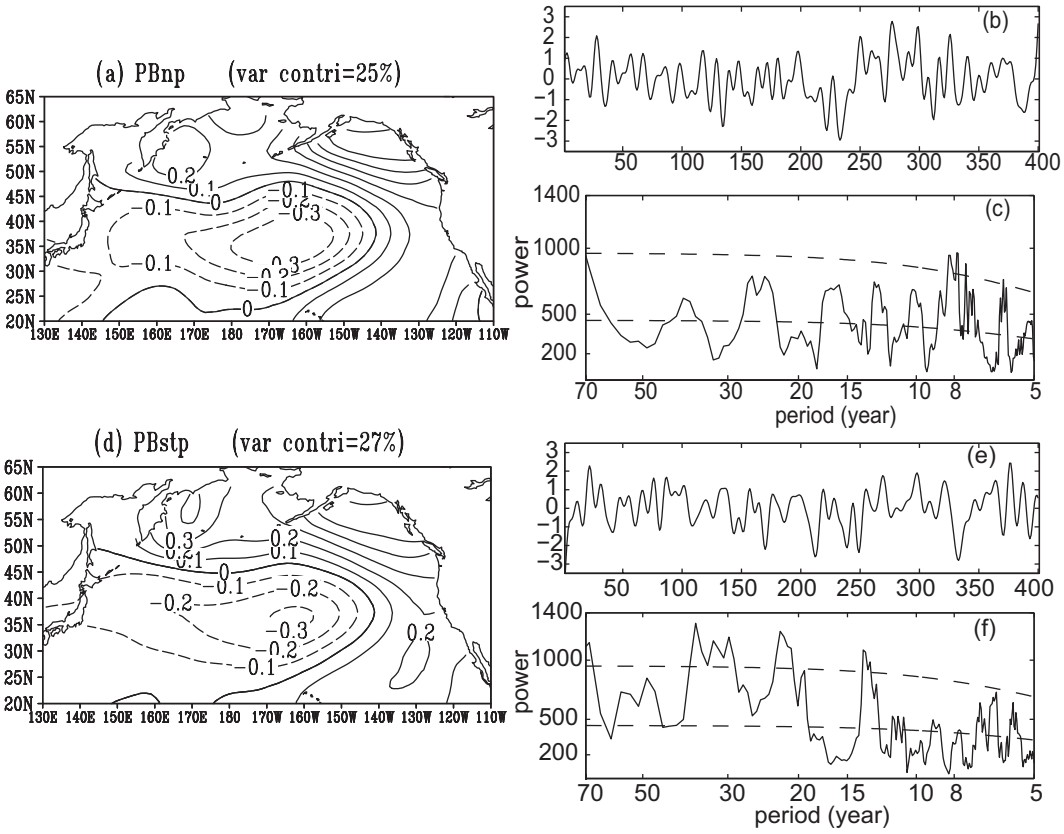

Fig. 8. The same as Fig. 4, but for SST in the FOAM Pbnp and Pbstp experiments.

where u is baroclinic zonal mean flow, W is the vertical velocity eigenvector, and the subscript z denotes the vertical derivation. The baroclininc Rossby wave speed c is the eigenvalue of Eq. (2).

5.3.1. *Ocean temperature and buoyancy frequency change*

Figure 9 shows North Pacific zonal mean temperature and buoyancy frequency (140°E–110°W), longitudinal mean temperature (20°–60°N), and their change between Ctrl and $2CO_2$. Under a warmer climate, the enhanced greenhouse effect permits the Earth's surface to absorb more radiation, so the upper ocean warms more than the deep ocean (Fig. 9b). The temperature increase in the high latitudes and west of the North Pacific Ocean is more than that in the low latitudes and in the east (Figs. 9b and d). Ocean buoyancy frequency, which is mainly influenced by temperature, also increases (ocean becomes more stable) (Fig. 9f). The buoyancy frequency (temperature) increase in the upper ocean is much more than that in the deep ocean, and that in the high latitudes much more than that in the low latitudes (Fig. 9f), so the baroclinic Rossby wave speed increase ratio is larger in the high latitudes (Fig. 10), according to Eq. (1). The more stable ocean suppresses vertical convection, allowing the upper ocean to warm more than the deep ocean, forming a positive feedback loop.

5.3.2. *Wave speed and transit time change*

Figure 10 shows North Pacific zonal mean first baroclinic Rossby wave speed, wave speed change ratio, transit time and transit time change ratio, in FOAM and the IPCC AR4 models experiments, with and without baroclinic zonal mean background flow. The results show that, under global warming: (1) the first baroclinic Rossby wave becomes faster and the transit time shortens; and (2) the wave speed increase ra-

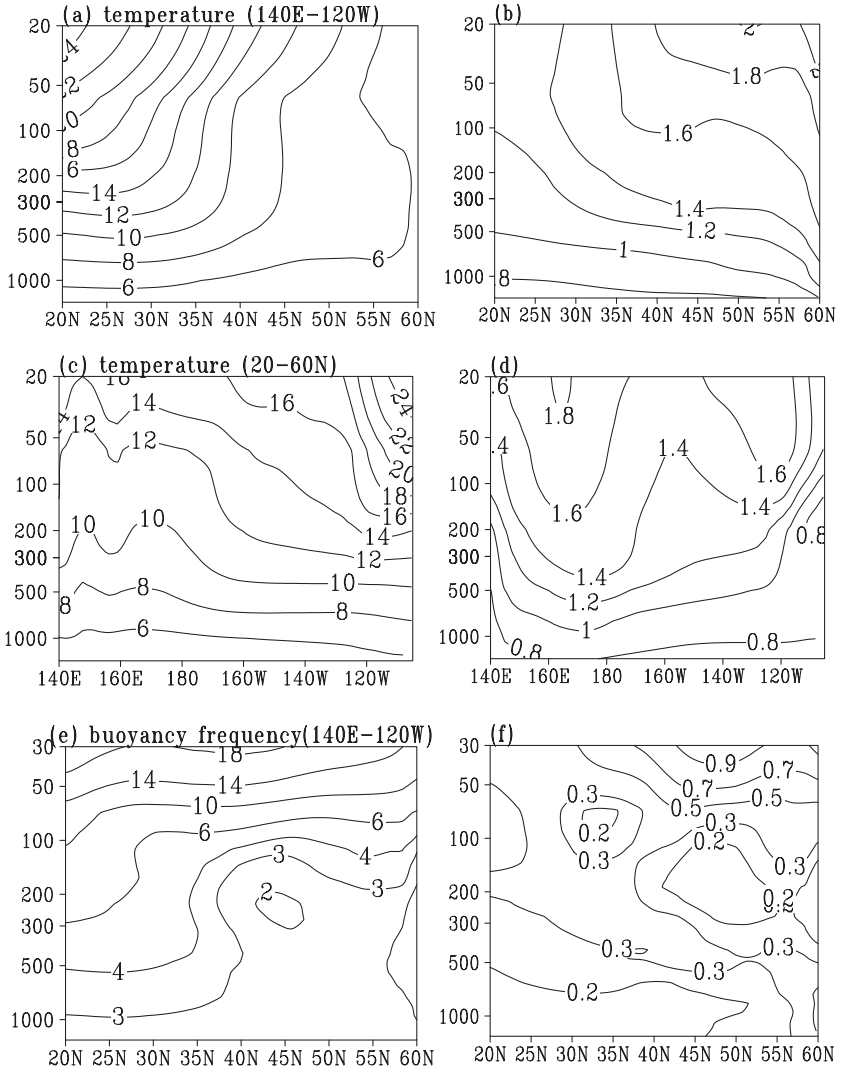

Fig. 9. North Pacific zonal mean temperature (140°E–120°W) (a, b), longitudinal mean temperature (20°–60°N) (c, d) (units: °C), and zonal mean buoyancy frequency (140°E–120°W) (e, f) (units: $10^{-3}S^{-1}$). The upper and lower panel figures are the Ctrl results and the difference between the Ctrl and $2CO_2$ results, respectively. The y-axis is the logarithm of depth (units: m).

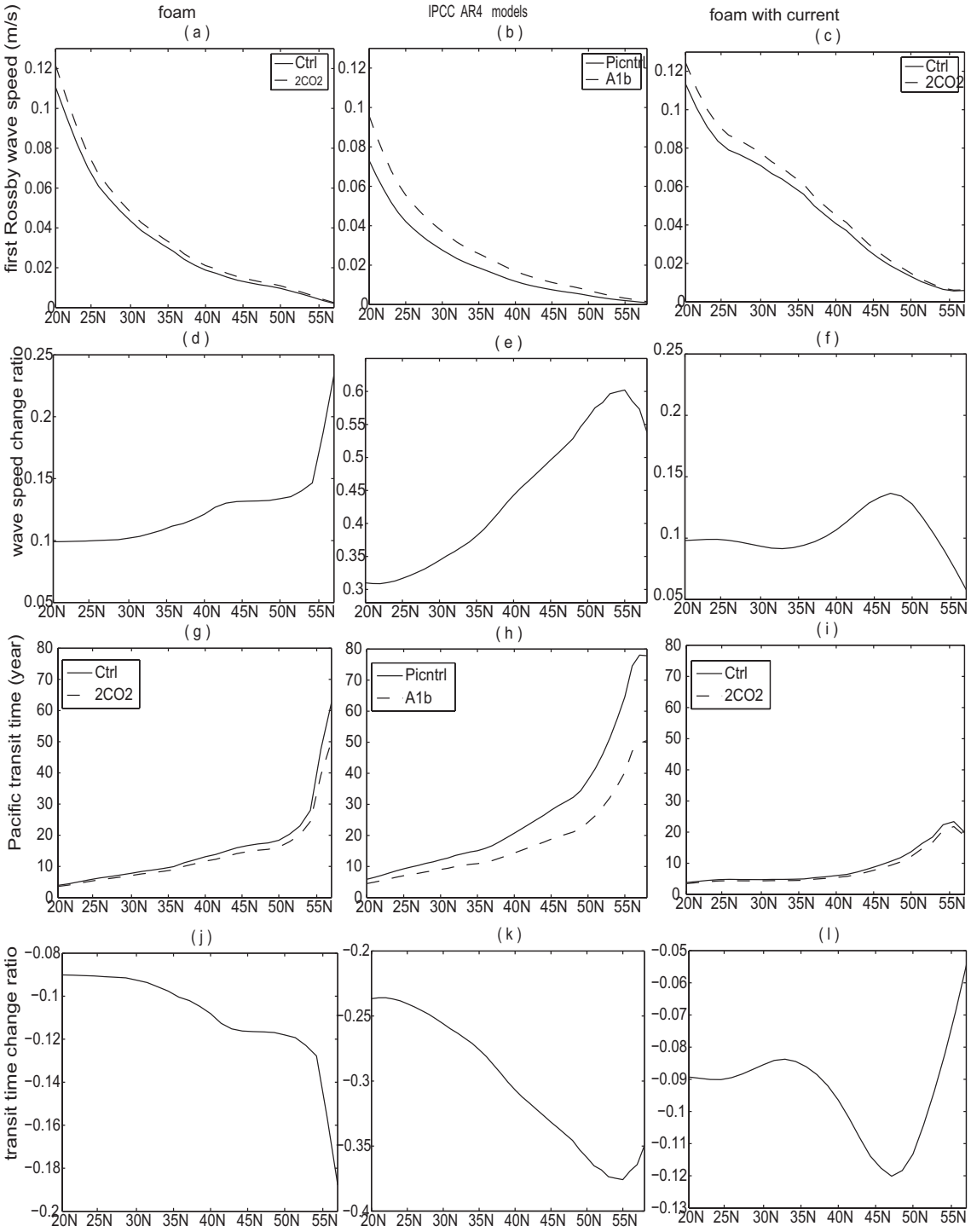

Fig. 10. North Pacific first baroclinic Rossby wave speed, transit time and their changes. Represented from the top to bottom, respectively, are North Pacific first baroclinic Rossby wave speed, wave speed change ratio, transit time, and transit time change ratio. Represented from left to right, respectively, are the results from the FOAM experiment, the 10 IPCC AR4 model experiments, and the FOAM experiment considering zonal current.

tio, transit time reduction and transit time reduction ratio of the first baroclinic Rossby wave in the high latitudes are much larger than those in the low latitudes.

According to Eq. (1), under a warmer climate, as ocean buoyancy frequency increases (Fig. 9d), the first oceanic baroclinic Rossby wave becomes faster (Figs. 10a–f) and the transit time shortens (Figs. 10g–i). Without baroclinic zonal mean flow, the *m*-order baroclinic Rossby wave speed increase is m^{-2} times the first baroclinic Rossby wave speed increase, but the *m*-order speed increase ratio is the same as the first baroclinic Rossby wave [see Eq. (1); figures not shown].

The first baroclinic Rossby wave speed increases by 10%

to 24% from 20°N to 55°N in $2CO_2$ compared to Ctrl (Fig. 10d), and by 31% to 60% from 20°N to 55°N in A1B compared to Picntrl (Fig. 10e). The first baroclinic Rossby wave transit time reduces by 9% to 16% from 20°N to 55°N in $2CO_2$ compared to Ctrl (Fig. 10j), and by 23% to 37% from 20°N to 55°N in A1B compared to Picntrl (Fig. 10k). The transit time reduction ratio (wave speed increase ratio) in the IPCC AR4 models is more obvious than that in FOAM at the same latitude (Fig. 10), because the CO_2 concentration increase ratio between Picntrl (290 ppm) and A1B (720 ppm) is larger than that between Ctrl (355 ppm) and $2CO_2$ (710 ppm; Table 1), which also supports the result that a warmer climate speeds up baroclinic Rossby waves and shortens their transit time.

5.4. *Rossby wave speed change and the PDO response*

North Pacific baroclinic Rossby wave adjustment is vital to the PDO period and SST amplitude, especially the baroclinic Rossby wave between 35°N and 60°N. The speeding up of baroclinic Rossby waves under a warmer climate causes the PDO to shift to a higher frequency, and North Pacific Ocean decadal variability and the PDO to become weaker. In addition, ocean buoyancy frequency increases (ocean stratification enhances) and baroclinic Rossby waves become faster (most obviously in the high latitudes) (section 5.3). As baroclinic Rossby waves speed up, the decadal variability (period $>$ 8 years) weakens, and so the PDO shifts to a higher frequency and becomes weaker. For example, if baroclinic Rossby waves speed up by 10 000 times under a much warmer climate, there will be no decadal variability (period $>$ 8 years) and PDO.

6. Conclusion and discussion

6.1. *Conclusion*

The PDO response to global warming in FOAM and IPCC AR4 model experiments was studied. The results showed that North Pacific Ocean decadal variability, its dominant mode (PDO), and atmosphere decadal variability get weaker under global warming, and the PDO shifts to a higher frequency.

Oceanic baroclinic Rossby wave adjustment is vital to the PDO, especially in the high latitudes. As the climate warms, ocean buoyancy frequency increases (ocean stratification enhances) and the baroclinic Rossby waves become faster. The oceanic baroclinic Rossby wave speed increase ratio and transit time reduction ratio in the high latitudes are much larger than those in the low latitudes. The faster baroclinic Rossby waves cause North Pacific Ocean decadal variability and the PDO to become weaker, and the PDO to shift to a higher frequency.

6.2. *Discussion*

Faster baroclinic Rossby waves might not be the exclusive reason for the shorter and weaker PDO under global warming. There are many possible PDO mechanisms, as mentioned in section 1 (Introduction), so there may well be another reason for the PDO weakening under global warming, such as North Pacific local ocean–atmosphere coupling and ocean circulation changes. Follow-up work from the present group will study the North Pacific local ocean–atmosphere coupling change and its role in weaker North Pacific Ocean decadal variability under global warming.

Owing to the long ocean memory, North Pacific Ocean decadal variability (local ocean–atmosphere coupling) influences atmospheric decadal variability, which has been investigated in many previous studies (Wu and Liu, 2003; Wu et al., 2003; Zhong and Liu, 2009). Therefore, the North Pacific Ocean decadal variability (North Pacific local ocean–atmosphere coupling) weakening might lead to atmospheric decadal variability weakening, which will be studied further.

Finally, in order to investigate the response of climate variability to global warming, it is suggested that the IPCC A1B experiment is run for as long as possible, such as to the year 2700, when the warmer climate with a CO_2 concentration of 720 ppm reaches a stable equilibrium.

Acknowledgements. This work was supported by the National Natural Science Foundation of China (NSFC) Creative Group Project (Grant No. 41221063) and Major Research Project (Grant No. 2013CB956200). The authors are grateful for Dr. LUO Dehai's suggestions, which were very helpful. Comments from three anonymous reviewers and the Editor were also greatly appreciated.

REFERENCES

An, S.-I., and B. Wang, 1999: Interdecadal change of the structure of the ENSO mode and its impact on the ENSO frequency. *J. Climate*, **13**, 2044–2055.

Biondi, F., G. Alexander, and D. R. Cayan, 2001: North Pacific decadal climate variability since 1661. *J. Climate*, **14**, 5–10.

Chelton, D. B., and M. Schlax, 1996: Global observations of oceanic rossby waves. *Science*, **272**, 234–238.

Chelton, D. B, R. A. DeSzoeke, M. G. Schlax, K. E. Naggar, and N. Siwertz, 1998: Geographical variability of the first baroclinic rossby radius of deformation. *J. Climate*, **28**, 433–460.

D'Arrigo, R., R. Villalba, and G. Wiles, 2001: Tree-ring estimate of pacific decadal climate variability. *Climate Dyn.*, **18**, 219–224.

Deser, C., A. S. Phillips, and J W. Hurrell, 2004: Pacific interdecadal climate variability: Linkages between the tropics and the North Pacific during boreal winter since 1900. *J. Climate*, **17**, 3109–3124.

D'Orgeville, M., and W. R. Peltier, 2009: Implications of both statistical equilibrium and global warming simulations with CCSM3. Part I: On the decadal variability in the North Pacific basin. *J. Climate*, **22**, 5277–5297.

Gershunov, A., and T. P. Barnett, 1998: Interdecadal modulation of ENSO teleconnections. *Bull. Amer. Meteor. Soc.*, **79**, 2715–2725.

Gu, D., and S. G. H. Philander, 1997: Interdecadal climate fluctuations that depend on exchanges between the tropics and extratropics. *Science*, **275**, 805–807.

Guilyardi, E., A. Wittenberg, A. Fedorov, M. Collins, C. Wang, A. Capotondi, G. J. Oldenborgh, and T. Stockdale, 2009: Un-

derstanding El Niño in ocean–atmosphere general circulation models: Progress and challenges. *Bull. Amer. Meteor. Soc.*, **90**, 325–340.

Hu, Z.-Z., and B. Huang, 2009: Interferential impact of ENSO and PDO on dry and wet conditions in the U.S. Great Plains. *J. Climate*, **22**, 6047–6065.

Huang, R. H., R. S. Cai, J. L. Chen, and L. T. Zhou, 2006: Interdecaldal variations of drought and flooding disasters in China and their association with the East Asian Climate System. *Chinese J. Atmos. Sci.*, **30**, 730–743.

Jacob, R. L., 1997: Low frequency variability in a simulated atmosphere–ocean system. Ph.D. dissertation, Dept. of Atmospheric and Oceanic Sciences, University of Wisconsin-Madison, 155 pp.

Jacobs, G. A., H. E. Hurlburt, J. C. Kindle, E. J. Metzger, J. L. Mitchell, W. J. Teague, and A. J. Wallcraft, 1994: Decade-scale trans-Pacific propagation and warming effects of an El Niño anomaly. *Nature*, **370**, 360–363.

Killworth, P. D., R. De Szoeke, and D. Chelton, 1997: The speed of observed and theoretical long extratropical planetary waves. *J. Phys. Oceanogr.*, **27**, 1946–1966.

Kleeman, R., J. P. McCreary Jr., and B. A. Klinger, 1999: A mechanism for generating ENSO decadal variability. *Geophys. Res. Lett.*, **26**, 1743–1746.

Kwon, Y. O., and C. Deser, 2007: North Pacific decadal variability in the community climate system model version 2. *J. Climate*, **20**, 2416–2433.

Latif, M., and T. P. Barnett, 1994: Causes of decadal climate variability over the North Pacific and North America. *Science*, **266**, 634–637.

Latif, M., and T. P. Barnett, 1996: Decadal climate variability over the North Pacific and North America: Dynamics and predictability. *J. Climate*, **9**, 2407–2423.

Liu, Z., L. Wu, R. Gallimore, and R. Jacob, 2002: Search for the origins of Pacific decadal climate variability. *Geophys. Res. Lett.*, **29**(10), 1404, doi: 10.1029/2001GL013735.

Mann, M. E., and J. M. Lees, 1996: Robust estimation of background noise and signal detection in climatic time series. *Climatic Change*, **33**, 409–445.

Mantua, N. J., and S. R. Hare, 2002: The Pacific decadal oscillation. *Journal of Oceanography*, **58**, 35–44.

Mantua, N. J., S. R. Hare, Y. Zhang, J. M. Wallance, and R. C. Francis, 1997: A Pacific decadal climate oscillation with impacts on salmon. *Bull. Amer. Metetor. Soc.*, **78**, 1069–1079.

Meehl, G. A., C. Covey, T. Delworth, M. Latif, B. McAvaney, J. F. B Mitchell, R. J. Stouffer, and K. E. Taylor, 2007: The WCRP CMIP3 multi-model dataset: A new era in climate change research. *Bull. Amer. Meteor. Soc.*, **88**, 1383–1394.

Merryfield, W. J., 2006: Changes to ENSO under CO_2 doubling in a multimodel ensemble. *J. Climate*, **19**, 4009–4027.

Miller, A. J., and N. Schneider, 2000: Interdecadal climate regime dynamics in the North Pacific Ocean: theories, observations and ecosystem impacts. *Progress in Oceanography*, **47**, 355–379.

Miller, A. J., F. Chai, S. Chiba, J. R. Moisan, and D. J. Neilson, 2004: Decadal-scale climate and ecosystem interactions in the North Pacific Ocean. *Journal of Oceanography*, **60**, 163–188.

Minobe, S., 1999: Resonance in bidecadal and pentadecadal climate oscillations over the North Pacific: Role in climatic regime shifts. *Geophys. Res. Lett.*, **26**, 855–858.

Münnich, M., M. Latif, S. Venzke, and E. Maier-Reimer, 1998: Decadal oscillations in a simple coupled model. *J. Climate*, **11**, 3309–3319.

Pierce, D. W., T. P. Barnett, N. Schneider, R. Saravanan, D. Dommenget, and M. Latif, 2001: The role of ocean dynamics in producing decadal climate variability in the North Pacific. *Climate Dyn.*, **18**, 51–70.

Rayner, N. A., D. E. Parker, E. B. Horton, C. K. Folland, L. V. Alexander, D. P. Rowell, E. C. Kent, and A. Kaplan, 2003: Global analyses of sea surface temperature, sea ice, and night marine air temperature since the late nineteenth century. *J. Geophys. Res.*, **108**, 4407–4443, doi: 10.1029/2002JD002670.

Saenko, O. A., 2006: Influence of global warming on baroclinic rossby radius in the ocean: A model intercomparison. *J. Climate*, **19**, 1354–1360.

Saravanan, R., and J. C. McWilliams, 1998: Advective ocean–atmosphere interaction: An analytical stochastic model with implications for decadal variability. *J. Climate*, **11**, 165–188.

Sato, Y., S. Yukimoto, H. Tsujino, H. Ishizaki, and A. Noda, 2006: Response of North Pacific ocean circulation in a Kuroshio-resolving ocean model to an arctic oscillation (AO)-like change in Northern Hemisphere atmospheric circulation due to greenhouse-gas forcing. *J. Meteor. Soc. Japan*, **84**, 295–309.

Schmittner, A., M. Latif, and B. Schneider, 2005: Model projections of the North Atlantic thermohaline circulation for the 21st century assessed by observations. *Geophys. Res. Lett.*, **32**, L23710, doi: 10.1029/2005GL024368.

Seager, R., Y. Kushnir, N. H. Naik, M. A. Cane, and J. Miller, 2001: Wind-driven shifts in the latitude of the Kuroshio–Oyashio extension and generation of SST anomalies on decadal timescales. *J. Climate*, **14**, 4249–4265.

Stouffer, R. J., and Coauthors, 2006: Investigating the causes of the response of the thermohaline circulation to past and future climate changes. *J. Climate*, **19**, 1365–1387.

Trenberth, K. E., and J. W. Hurrell, 1994: Decadal atmosphere-ocean variations in the Pacific. *Climate Dyn.*, **9**, 303–319.

Wang, B., 1995: Interdecadal changes in El Niño onset in the last four decades. *J. Climate*, **8**, 267–285.

Wu, L., and Z. Liu, 2003: Decadal variability in the North Pacific: The eastern orth Pacific mode. *J. Climate*, **16**, 3111–3131.

Wu, L., Z. Liu, R. Gallimore, R. Jacob, D. Lee, and Y. Zhong, 2003: Pacific decadal variability: The tropical pacific mode and the North Pacific mode. *J. Climate*, **16**, 1101–1120.

Wu, L., Z. Liu, C. Li, and Y. Sun., 2007: Extratropical control of recent tropical Pacific decadal climate variability: A relay teleconnection. *Climate Dyn.*, **28**, doi: 10.1027/s00382-006-0198-5.

Yin, J. H., 2005: A consistent poleward shift of the storm tracks in simulations of 21st century climate. *Geophys. Res. Lett.*, **32**, L18701, doi: 10.1029/2005GL023684.

Zhong, Y., and Z. Liu, 2009: On the mechanism of pacific multi-decadal climate variability in CCSM3: The role of the subpolar North Pacific ocean. *J. Phys. Oceanogr.*, **39**, 2052–2076.